Acoustic modeling using a three-dimensional coupled-mode model

Megan S. Ballard
Applied Research Laboratories at the University of Texas at Austin
Environmental Science Laboratory
Austin, Texas 78758
phone: (512) 835-3953 fax: (512) 490-4225 email: meganb@arlut.utexas.edu

LONG-TERM GOALS

The over-all goal of this research is the development of an accurate and reliable propagation model applicable to environments which exhibit strong range dependence in all three spatial dimensions.

OBJECTIVES

The objective of this work is to gain an understanding the physics of propagation in continental shelf areas, specifically horizontal refraction and mode coupling induced by three-dimensional (3D) inhomogeneities in the waveguide. A coupled-mode approach has been applied for this purpose. The coupled-mode approach is attractive for solving problems involving 3D propagation for several reasons. First, this technique provides intuitive results for understanding the features responsible for observed propagation effects in range-dependent environments. For example, upslope propagation is characterized by acoustic energy radiated into the bottom at discrete depths associated with mode cut-off. The modal decomposition of the acoustic field has also been used to describe horizontal refraction in a wedge-shaped ocean, for which the single-mode interference pattern associated with rays launched up and across the shelf has been well documented [Weinberg and Burridge (1974)]. Furthermore, coupled-mode solutions can be highly accurate and have been used for benchmarking solutions to range-dependent problems [Jensen and Ferla (1990)]. In order to appreciate the limitations of existing 3D models, it is necessary to have methods which can provide reference solutions for comparison.

APPROACH

A 3D acoustic propagation model based on the stepwise coupled-mode approach [Evans (1983)] implemented as a single-scatter solution has been developed. This technique is based on a hybrid modeling approach for which normal modes supply the vertical dependence and a parabolic equation (PE) solution provides the horizontal dependence. The inhomogeneous Helmholtz equation for pressure $P(r, \theta, z)$ at range r, azimuth θ, and depth z from a point continuous wave source of amplitude $S(\omega)$,

Report Documentation Page

1. REPORT DATE **30 SEP 2013**	2. REPORT TYPE	3. DATES COVERED **00-00-2013 to 00-00-2013**
4. TITLE AND SUBTITLE **Acoustic modeling using a three-dimensional coupled-mode model**		5a. CONTRACT NUMBER
		5b. GRANT NUMBER
		5c. PROGRAM ELEMENT NUMBER
6. AUTHOR(S)		5d. PROJECT NUMBER
		5e. TASK NUMBER
		5f. WORK UNIT NUMBER
7. PERFORMING ORGANIZATION NAME(S) AND ADDRESS(ES) **University of Texas at Austin,Applied Research Laboratories,Environmental Science Laboratory,Austin,TX,78758**		8. PERFORMING ORGANIZATION REPORT NUMBER
9. SPONSORING/MONITORING AGENCY NAME(S) AND ADDRESS(ES)		10. SPONSOR/MONITOR'S ACRONYM(S)
		11. SPONSOR/MONITOR'S REPORT NUMBER(S)

12. DISTRIBUTION/AVAILABILITY STATEMENT
Approved for public release; distribution unlimited

13. SUPPLEMENTARY NOTES

14. ABSTRACT

15. SUBJECT TERMS

16. SECURITY CLASSIFICATION OF:			17. LIMITATION OF ABSTRACT	18. NUMBER OF PAGES	19a. NAME OF RESPONSIBLE PERSON
a. REPORT **unclassified**	b. ABSTRACT **unclassified**	c. THIS PAGE **unclassified**	**Same as Report (SAR)**	**10**	

located at range $r = 0$ and depth $z = z_0$, is given by

$$\rho(r,\theta,z)\nabla \cdot \left[\frac{1}{\rho(r,\theta,z)}\nabla P(r,\theta,z)\right] + k^2(r,\theta,z)P(r,\theta,z) = -4\pi S(\omega)\frac{\delta(r)}{r}\delta(z-z_0), \tag{1}$$

where $\nabla = \hat{\mathbf{r}}\frac{\partial}{\partial r} + \hat{\theta}\frac{1}{r}\frac{\partial}{\partial \theta} + \hat{\mathbf{z}}\frac{\partial}{\partial z}$ is the gradient operator in cylindrical coordinates, $k(r,\theta,z) = \omega/c(r,\theta,z)$ is the acoustic wavenumber, $\omega = 2\pi f$, f is the acoustic frequency, $c(r,\theta,z)$ is sound speed, and $\rho(r,\theta,z)$ is density. In this work, the range-dependent environment is approximated by a number of range-independent regions defined in the range-bearing plane. In the discrete environment, the continuous variables of Eq. (1) are discretized in range and bearing such that the range-independent region at the ith step in range and j^{th} step in azimuth is characterized by sound speed $c_{i,j}(z)$, density $\rho_{i,j}(z)$, and wavenumber $k_{i,j}(z)$. The solution for pressure in the ith step in range is found by a separation of variables

$$P_i(r,\theta,z) = \sum_{m=1}^{M} A_{m_i}(r,\theta)\phi_{m_{i,j}}(z) \text{ for } r_{i-1} < r < r_i, \tag{2}$$

where $A_{m_i}(r,\theta)$ are the modal amplitudes in the ith step in range, and $\phi_{m_{i,j}}(z)$ are the modal eigenfunctions in the ith step in range and j^{th} step in azimuth. As denoted by Eq. (2), the modal amplitudes are continuous functions of range and azimuth whereas modal eigenfunctions are continuous functions in depth only.

The modal eigenfunctions $\phi_{m_{i,j}}(z)$ are defined locally in each range-independent region such that they satisfy

$$\rho_{i,j}(z)\frac{\partial}{\partial z}\left[\frac{1}{\rho_{i,j}(z)}\frac{\partial \phi_{m_{i,j}}(z)}{\partial z}\right] + \left[k_{i,j}^2(z) - k_{m_{i,j}}^2\right]\phi_{m_{i,j}}(z) = 0, \tag{3}$$

where $k_{m_{i,j}}$ is the horizontal wavenumber of the mth mode. Within each region, the environment consists of an arbitrary number of fluid layers bounded above by a pressure release surface and below by a fluid half-space. In this work, the Pekeris branch cut is chosen such that the total pressure is calculated from a Pekeris branch line integral, plus a finite sum of trapped modes, plus an infinite sum of leaky modes. A small gradient is introduced in the lower half-space which effectively removes the branch point and associated branch cut from the problem [Westwood and Koch (1999)].

In the solution for the modal amplitudes, environmental range dependence takes place discretely at the interfaces between regions. Within the ith step in range, the environment varies as a function of azimuth only, and the modal amplitudes satisfy the 2D Helmholtz equation

$$\frac{1}{r}\frac{\partial}{\partial r}\left(r\frac{\partial A_{m_i}(r,\theta)}{\partial r}\right) + \frac{1}{r^2}\frac{\partial^2 A_{m_i}(r,\theta)}{\partial \theta^2} + k_{m_{i,j}}^2 A_{m_i}(r,\theta) = 0 \text{ for } r_{i-1} < r < r_i. \tag{4}$$

This equation must be solved for each mode with the horizontal refraction determined by the modal phase speed $c_{m_{i,j}}^{\text{ph}} = \omega/\text{Re}\{k_{m_{i,j}}\}$ and modal attenuation $\alpha_{m_{i,j}} = \text{Im}\{k_{m_{i,j}}\}$. The solution is obtained from a PE model [Collins (1994)] by factoring Eq. (4) and keeping the outgoing factor to obtain

$$\frac{\partial A_{m_i}(r,\theta)}{\partial r} = ik_0\sqrt{1 + k_0^{-2}\left(\frac{1}{r^2}\frac{\partial^2}{\partial \theta^2} + k^2 - k_0^2\right)}A_{m_i}(r,\theta) \text{ for } r_{i-1} < r < r_i, \tag{5}$$

where $k_0 = \frac{\omega}{c_0}$ is the reference wavenumber, and c_0 is the reference sound speed. Equation (5) differs from the original PE model which is defined in the range-depth plane with pressure release boundary

conditions at the top and bottom of the waveguide. The starting function is a delta function located at the origin with amplitude determined by the source depth and the modal eigenfunctions in region $i = 1$,

$$A_{m_1}(0, \theta) = 4\pi S(\omega) \frac{\phi_{m_{1,j}}(z_0)}{\rho_{1,j}(z_0)}. \tag{6}$$

In the stepwise coupled-mode model, mode coupling is calculated in the outgoing direction at the interfaces between the range-independent regions. Azimuthal mode coupling is neglected, such that the mode-coupling occurs only through the boundary conditions at interfaces defined in the tangential direction. The two-way coupled-mode solution is obtained by requiring continuity of pressure and particle velocity at $r = r_j$ located at the boundary between the (i, j) and $(i+1, j)$ range-independent regions. In this work, the backscattered field is neglected to obtain the single-scatter solution

$$A_{m_{i+1}}(r_i, \theta) = \frac{1}{2} \sum_{n=1}^{M} \left[\int_{-\infty}^{\infty} \frac{\phi_{n_{i,j}}(z)\phi_{m_{i+1,j}}(z)}{\rho_{i+1,j}(z)} dz + \frac{k_{n_{i,j}}}{k_{m_{i+1,j}}} \int_{-\infty}^{\infty} \frac{\phi_{n_{i,j}}(z)\phi_{m_{i+1,j}}(z)}{\rho_{i,j}(z)} dz \right] A_{n_i}(r_i, \theta). \tag{7}$$

WORK COMPLETED

The main accomplishments of 2013 include: (1) a comparison of the 3D coupled-mode solution to a finite element method (FEM) solution, (2) ranging estimates from horizontal multipath in a continental shelf environment, (3) modeling of 3D propagation effects observed in the Church Stroke III data set, and (4) development of a robust normal mode code for environments with elastic layers.

RESULTS

Comparison of the 3D coupled-mode solution to a FEM solution

As described above, in formulating the 3D coupled-mode solution, it was assumed that mode-coupling in the azimuthal direction is small and can be neglected. The effects of this assumption are examined by comparing the solution from the 3D coupled-mode model to a solution obtained using a FEM model applied with the longitudinally invariant (LI) technique. This technique is appropriate for environments which have lateral variations that occur in one dimension only. The solution is obtained by applying a cosine transform to eliminate the range-independent dimension [Isakson and Chotiros (2011); Goldsberry and Isakson (2013)].

The propagation environment consists of an isovelocity water column ($c = 1500$ m/s, $\rho = 1.0$ g/cm^3) over an acoustic half-space having the properties of sand ($c = 1767.3$ m/s, $\rho = 1.845$ g/cm^3, $\alpha = 0.75225$ dB/λ). The only range-dependent feature is a cosine-shaped hill that extends infinitely in the y-direction, such that the water depth $d(x)$ is defined by

$$d(x) = \begin{cases} 47.5 - 12.5\cos(\frac{2\pi x}{500}) & \text{if } 2750 \le x \le 3250 \\ 60 & \text{if } x < 2750 \text{ or } x > 3250. \end{cases} \tag{8}$$

The solution was calculated for a source located at a depth of 20 m and a frequency of 100 Hz. The infinite cosine hill induces strong horizontal refraction and mode-coupling effects. This is demonstrated by comparisons to N×2D coupled-mode and 3D adiabatic-mode solutions in Fig. 1(a) and (b), respectively.
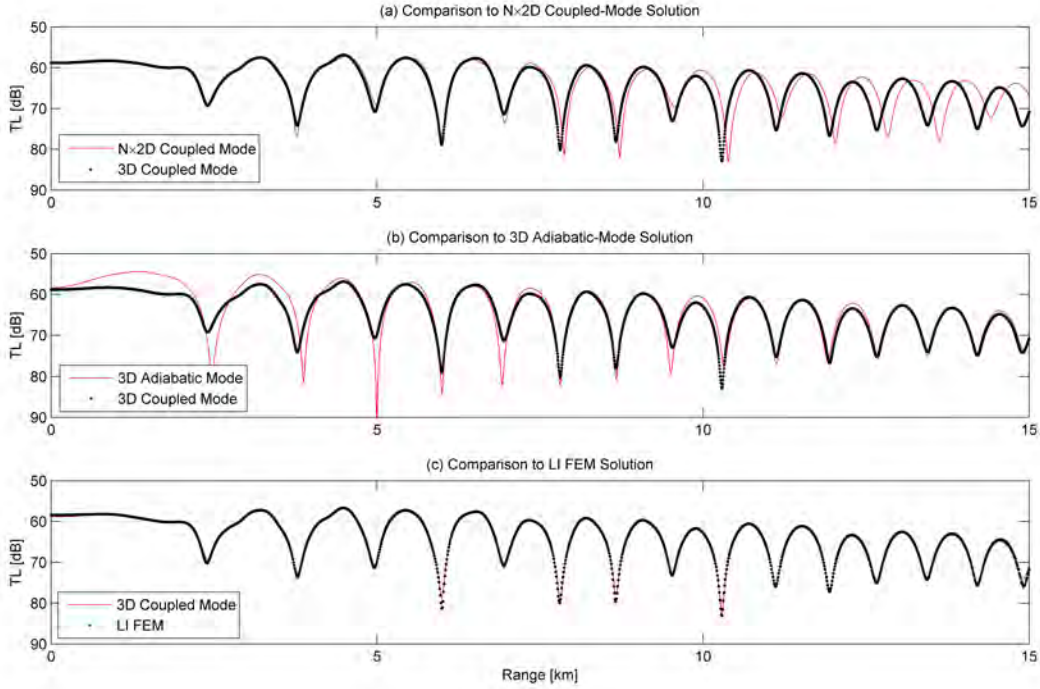
3

Figure 1: Comparison of the 3D coupled-mode solution at a depth of 20 m along x = 5 km to solutions calculated by (a) N×2D adiabatic-mode technique and by (b) 3D adiabatic-mode technique to demonstrate the relative importance of these effects. Comparison of the 3D coupled-mode solution to a solution calculted using the FEM with LI technique to demonstrate solution accuracy.

The 3D coupled-mode solution for transmission loss (TL) over the infinite cosine hill at a depth of 20 m along $x = 5$ km is compared to the solution calculated by the LI technique with the FEM in Fig. 1(c). With the exception of the nulls in the TL curves, the solutions are within 0.5 dB. This error is on the same order as the error in 2D solutions calculated for propagation over the axisymmetric cosine hill. Therefore, the error in the 3D solutions is attributed to the intrinsic differences in the approaches used to solve the 2D propagation problem. Hence, the assumption of negligible azimuthal mode coupling was validated for this environment.

Ranging estimates from horizontal multipath in a continental shelf environment

This work seeks to exploit horizontal multipath effects measured in beamformed data from a horizontal line array (HLA) to estimate the range of an acoustic source. A normal mode approach is applied, and rays are traced in the horizontal plane with refraction determined by the modal phase speed. The technique is applied to acoustic data recorded on 22 February 2009 by an HLA located 12 km east of the southern coast of Florida. The array was oriented downslope, providing a broadside look along the 250 m isobath. During the experiment, the *R/V Walton Smith* towed a source broadcasting a 2-minute sequence of signals [Heaney and Murray (2009)]. The source was towed at a depth of 100 m as the *R/V Walton Smith* traveled north-northwest, parallel to the Florida coastline until it was approximately 63 km north of the array. The ship then turned around and towed the source at a depth of 20 m as it traveled back south-southeast along the same path.
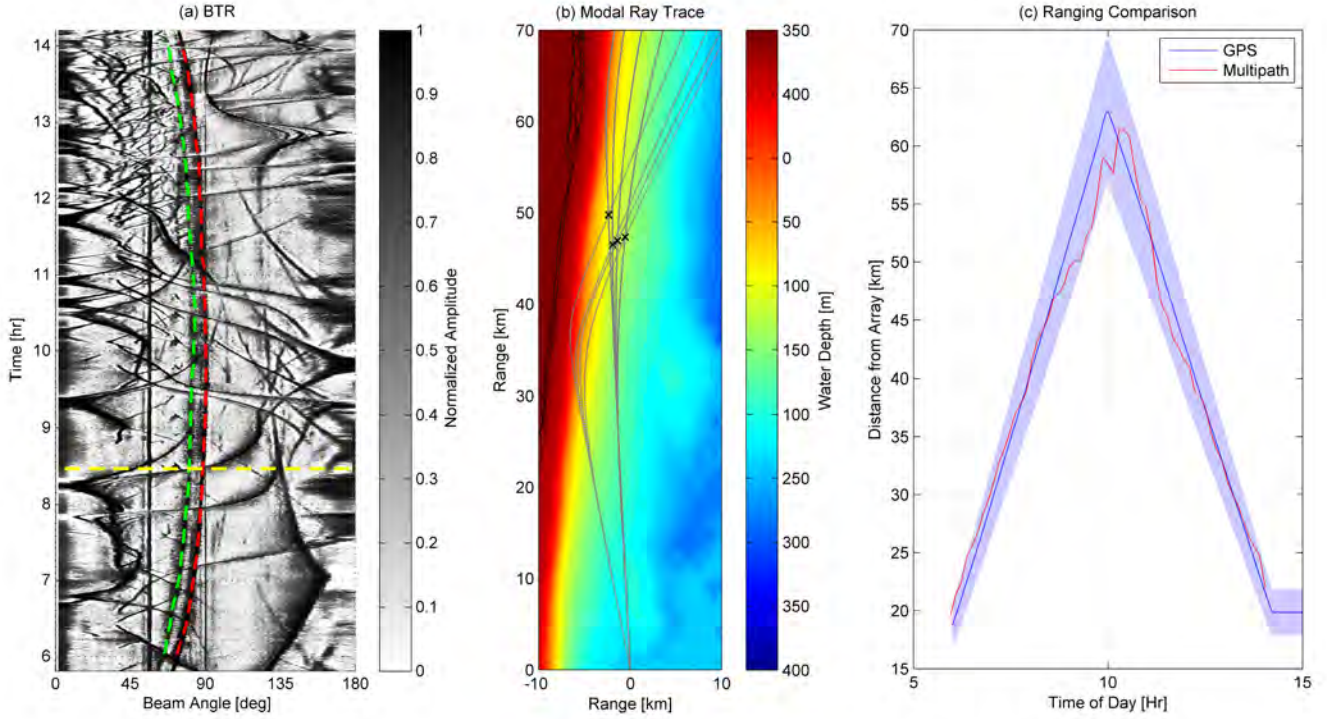
Figure 2: (a) BTR with bearing angles of the direct and refracted paths highlighted by the dashed lines. The horizontal dashed line at time 08:38 indicates the data used for additional analysis. (b) Horizontal ray traces for modes one through four at 50 Hz overlaid on bathymetry. The x- and y-axes are distance relative to the array location. (c) Comparison of estimated source range using the multipath ranging technique to calculated range using GPS data. The shaded region represents 10% ranging error referenced to the GPS data.

A bearing time record (BTR) of the data is displayed in Fig. 2(a). The bearing angles of the direct and refracted paths of the signal broadcasted by the towed source are highlighted by the dashed lines. To illustrate the multipath ranging technique, the horizontal ray trace for a single time scan is shown in Fig. 2(b). The time selected for this analysis is 08:38 and is indicated by the horizontal dashed line in Fig. 2(a). At this time, the estimated bearing angles of the direct and refracted paths were 86.63º and 78.57º, respectively. The ray trace was performed using the modal phase speed for modes one through four at 50 Hz to determine the refraction of the rays. The rays traced for the direct and refracted paths are shown by the solid and dashed lines, respectively, for all four modes. The location of the source is estimated from the intersection of the rays, marked by the "x's" in Fig. 2(b).

The procedure described above was repeated for 60 estimates of the direct and refracted bearing angles over an eight hour period to build up a track of the source's location over time. For this application, the modal phase speed corresponding to mode three at 50 Hz was used. The ranging estimate is presented in Fig. 2(c). The largest errors in the estimate occur when the source is farthest away from the array and lower SNR has degraded the accuracy of the estimated bearing angles. For this result, the average of the absolute error in the range estimate is 3.7%, and the error does not exceed 10% at any range.
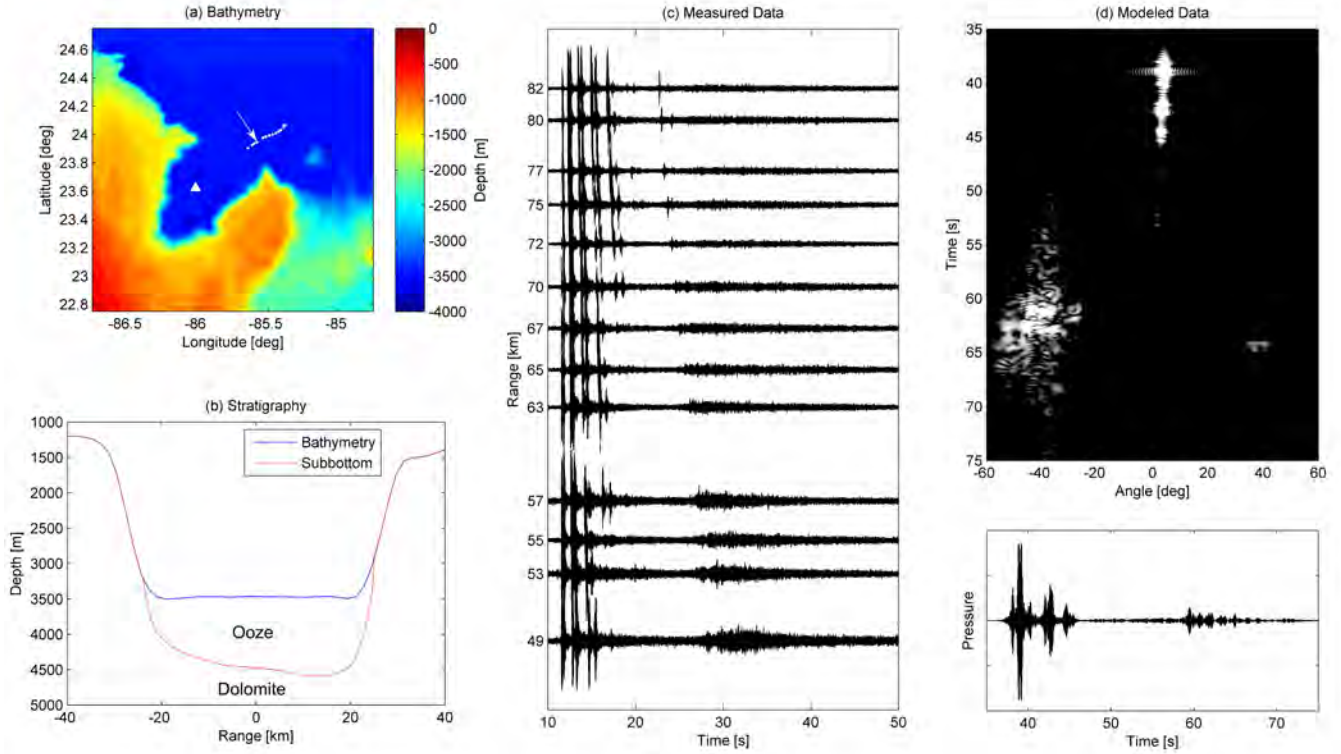
5

Figure 3: (a) Bathymetry of the Catoche Tongue with the location of the ACODAC array (triangle) and SUS charges (dots). (b) Reconstructed stratigraphy of the Catoche Tongue along a northwest transect passing through the ACODAC array location with the array located at 0 km and positive ranges oriented to the southeast. (c) Data recorded on channel 11 of the ACODAC array from the 13 SUS charges deployed at the locations indicated in Fig. 3(a). The y-axis is distance from the SUS charge to the ACODAC array. (d) Modeled data for the SUS charge located 57 km away from the ACODAC array beamformed with a HLA orientated with 90⁰ in the northwest direction.

Modeling of 3D propagation effects observed in the Church Stroke III data set

Three dimensional horizontally refracted arrivals recorded in the Catoche Tongue region of the Gulf of Mexico as part of the Church Stroke III Exercise in 1979 were modeled. Acoustic data from the Acoustic Data Capsule (ACODAC) vertical line array (VLA), located in the center of the tongue, as shown in Fig. 3(a), were recently recovered as part of the Long-Range Acoustic Propagation Project (LRAPP) tape recovery effort. The ACODAC array was moored at 23.62° N, 86.02° W in approximately 3470 m of water. During the exercise, 361 Signal Underwater Sound (SUS) charges were deployed. A subset of 13 shots located nearest the array were examined in this work, and their locations are indicated in Fig. 3(a). Sagers and Ballard (2013) assessed the stratigraphic structure of the seabed was from seismograms and core data [Buffler et al. (1984); Worzel (1973); Shaub (1987); Brunson et al. (1980)]. Fig. 3(b) shows the geoacoustic representation used for the propagation modeling.

The time series for the SUS events recorded on channel 11 (945 m depth) are shown in Fig. 3(c). The first arrival for each event has been aligned at 10 s. The direct (non-horizontally refracted) arrivals are received within the first 10 seconds after the first arrival. A later set of horizontally refracted arrivals are

6

also present in every SUS event with the arrival time increasing as the SUS range decreases. The later arrivals also appear to become more diffuse as the SUS range decreases.

The acoustic data were modeled in a 5 Hz band centered at 25 Hz using a hybrid 3D adiabatic-mode approach [Ballard (2012)]. The modeled data for the SUS charge located 57 km from the ACODAC array (indicated by the arrow in Fig. 3(a)) are shown in Fig. 3(d). The modeled data were beamformed with a HLA orientated with broadside look in the southwest direction. The beamformed data clearly show the direct path arrival at angle of approximately 5º with a strong refracted arrival at later times between -60º and -20º and a weak refracted arrival at approximately 40º. The strong refracted arrival is caused by interaction with the southern slope of the Catoche Tongue while the weak refracted arrival results from interaction with the northern slope. The relative strength of the refracted arrivals is caused by the comparative steepness of the southern slope and by its proximity to the SUS charges.

Development of normal mode code for environments with elastic layers

A robust normal mode code for calculating the eigenvalues and eigenfunctions in environments with elastic layers using a FEM approach is under development. In this solution, the environment is assumed to be made up of a number of layers with constant density ρ and shear wave speed c_s. The compressional wave speed c_p is allowed to vary within a layer. Within each layer, the shear ψ and compressional ϕ potentials satisfy

$$\nabla^2 \phi = \frac{1}{c_p^2} \frac{\partial^2 \phi}{\partial t^2}, \quad \nabla^2 \psi = \frac{1}{c_s^2} \frac{\partial^2 \psi}{\partial t^2}.$$

(9)

The displacements and stresses can be written in terms of the potentials as

$$u(r,z) = \frac{\partial \phi}{\partial r} + \frac{\partial^2 \psi}{\partial r \partial z}, \qquad\qquad w(r,z) = \frac{\partial \phi}{\partial z} - \frac{1}{r} \frac{\partial}{\partial r} r \frac{\partial \psi}{\partial r},$$

$$\sigma_{zz}(r,z) = (\lambda + 2\mu) \frac{\partial w}{\partial z} + \lambda \frac{1}{r} \frac{\partial (ru)}{\partial r}, \qquad\qquad \sigma_{rz}(r,z) = \mu \left(\frac{\partial u}{\partial z} + \frac{\partial w}{\partial r} \right),$$

$$\sigma_{rr}(r,z) = \lambda \left(\frac{1}{r} \frac{\partial}{\partial r}(ru) + \frac{\partial w}{\partial z} \right) + 2\mu \frac{\partial u}{\partial r}, \qquad\qquad \sigma_{\phi\phi}(r,z) = \lambda \left(\frac{1}{r} \frac{\partial}{\partial r}(ru) + \frac{\partial w}{\partial z} \right) + 2\mu \frac{u}{r}.$$

where λ and μ are the Lamé constants.

Solutions to range-dependent problems will be calculated using the stepwise coupled-mode approach described above with boundary conditions defined by the momentum conservation equations [Koch et al. (1983)]

$$\rho \frac{\partial^2 u}{\partial t^2} = \frac{1}{r} \frac{\partial}{\partial r}(r\sigma_{rr}) + \frac{\partial \sigma_{rz}}{\partial z} - \frac{1}{r} \sigma_{\phi\phi},$$

$$\rho \frac{\partial^2 w}{\partial t^2} = \frac{1}{r} \frac{\partial}{\partial r}(r\sigma_{rz}) + \frac{\partial^2 \sigma_{zz}}{\partial z^2}.$$

IMPACT/APPLICATIONS

The impact of this work is an increased understanding of acoustic propagation through complicated coastal environments for which the bathymetry, seabed properties, and oceanography can vary in three dimensions.

TRANSITIONS

The primary transition for this project is an accurate and reliable model for acoustic propagation in environments with strong three-dimensional range dependence. Because coupled-mode approaches are computationally intensive, they have historically been used to benchmark faster techniques which approximate the solution to the wave equation.

RELATED PROJECTS

Geoacoustic inversion in three-dimensional environments

The goal of this project is to estimate water column sound speed in a 3D volume using modal travel time measurements from multiple source-receiver pairs. A thorough understanding of the forward problem, including the effects of horizontal refraction and mode coupling, is necessary to successfully estimate environmental parameters in regions with 3D inhomogeneities. This project is currently funded by ARL:UT's IR&D program.

Acoustic propagation modeling for diver detection sonar systems

The purpose of this work is to characterize waveforms at virtual receiver distances on the order of a 1000 meters away from active diver detection sonar systems installed at fixed locations within operational sites of interest. The 3D coupled-mode model is applied for this purpose. This project is funded by Space and Naval Warfare Systems Center Pacific.

REFERENCES

M. S. Ballard. Modeling three-dimensional propagation in a continental shelf environment. *J. Acoust. Soc. Am.*, 131(3):1969–1977, 2012.

B. A. Brunson, M. M. Truxillo, and R. B. Evans. Environmental effects on low frequency transmission loss in the Gulf of Mexico. Technical report, Naval Ocean Research Development Activity, 1980.

R. T. Buffler, W. Schlager, and K. A. Pisciotto. Internal Reports, Deep Sea Drilling Project. *US Government*, 77(Site 536), 1984.

M. Collins. Generalization of the split-step Pade solution. *J. Acoust. Soc. Am.*, 96:382–385, 1994.

R. B. Evans. A coupled mode solution for acoustic propagation in a waveguide with stepwise depth variations of a penetrable bottom. *J. Acoust. Soc. Am.*, 74(1):188–195, 1983.

B. M. Goldsberry and M. Isakson. Comparison of two-dimensional axial-symmetric and longitudinally invariant methods for three-dimensional shallow water acoustic propagation using finite element methods. In *POMA 19*, page 070080, 2013.

K. D. Heaney and J. J. Murray. Measurement of three-dimensional propagation in a continental shelf environment. *J. Acoust. Soc. Am.*, 125(3):1394–1402, 2009.

M. Isakson and N. Chotiros. Modeling the effects of boundary roughness on transmission loss measurements in shallow water waveguides using finite elements. In *Underwater Acoustic Measurements: Technologies and Results, 4th International Conference, Kos, Greece*, 2011.

F. B. Jensen and C. M. Ferla. Numerical solutions of range-dependent benchmark problems in ocean acoustics. *J. Acoust. Soc. Am.*, 87(4):1499–1510, 1990.

R. A. Koch, C. Penland, P. J. Vidmar, and K. E. Hawker. On the calculation of normal mode group velocity and attenuation. *J. Acoust. Soc. Am.*, 73(3):820–825, 1983.

J. D. Sagers and M. S. Ballard. Sediment structure near the Church Stroke III Exercise Region, Including the Catoche Tongue. Technical Report ARL-TL-EV-13-69, Applied Research Laboratories at the University of Texas at Austin, 2013.

F. J. Shaub. The Catoche Tongue: An example of Mesozoic rift and subsidence episodes in the Gulf of Mexico. In *Offshore Technology Conference*, 1987.

H. Weinberg and R. Burridge. Horizontal ray theory for ocean acoustics. *J. Acoust. Soc. Am.*, 55(1): 63–79, 1974.

E. K. Westwood and R. A. Koch. Elimination of branch cuts from the normal-mode solution using gradient half spaces. *J. Acoust. Soc. Am.*, 106(5):2513–2523, 1999.

L. Worzel. Internal Reports, Deep Sea Drilling Project. *US Government*, 77(Site 95), 1973.

PUBLICATIONS

Refereed Journal Articles

Christopher M. Bender, Megan S. Ballard, and Preston S. Wilson, "The effects of environmental variability and spatial sampling on the solution of the three-dimensional linearized inversion problem for ocean sound speed,"*Journal of the Acoustical Society of America*. [in review]

Megan S. Ballard, Benjamin M. Goldsberry, and Marcia J. Isakson,"A three-dimensional propagation model with stepwise coupled modes," *Journal of the Acoustical Society of America*. [in review]

Megan S. Ballard,"Estimation of source range using horizontal multipath in continental shelf environments," *Journal of the Acoustical Society of America*, **134**(4), EL340-EL344, 2013.

Conference Proceedings

Megan S. Ballard, "An assessment of the importance of azimuthal mode coupling in three-dimensional acoustic propagation modeling," *Underwater Acoustics Conference*, 2013.

Megan S. Ballard, "Three-dimensional acoustic propagation under a rough sea surface," *Proceedings of Meetings on Acoustics*, Vol. 19, pp. 070077, 2013.

Technical Reports

Jason D. Sagers and Megan S. Ballard, "Sediment Structure near the Church Stroke III Exercise Region, Including the Catoche Tongue," ARL-TL-EV-13-69, Applied Research Laboratories at the University of Texas at Austin, 2013.

Presentations

Megan S. Ballard, "An assessment of the importance of azimuthal mode coupling in three-dimensional acoustic propagation modeling," *Underwater Acoustics Conference*, Corfu, Greece, June, 2013.

Megan S. Ballard, "Three-dimensional acoustic propagation under a rough sea surface," 165th Meeting of the Acoustical Society of America, Montreal, Canada, June, 2013.

Chris M. Bender, Megan S. Ballard, and Preston S. Wilson, "Range and cross-range resolution from a three-dimensional linearized perturbative inversion scheme," 164th Meeting of the Acoustical Society of America, Kansas City, Missouri, October, 2012.